The Fourth China-Japan-Korea Joint Symposium on Optimization of Structural and Mechanical Systems
Kunming, Nov. 6-9, 2006, China

SHAPE OPTOMIZATION OF H-BEAM FLANGE FOR MAXIMUM PLASTIC ENERGY DISSIPATION

Makoto Ohsaki[1]*, Peng Pan[2]

[1]*Dept. of Architecture and Architectural Engineering, Kyoto University,*
Kyotodaigaku-Katsura, Nishikyo, Kyoto 615-8540, Japan
** Corresponding author:ohsaki@archi.kyoto-u.ac.jp*
[2]*Disaster Prevention Research Institute, Kyoto University*
Gokasho, Uji 611-0011, Japan

Abstract
Optimal shapes are found for the flange of an H-beam. A forced displacement is given at the free end of the cantilever beam so that the average deformation angle reaches the specified value. The objective function to be maximized is the dissipated energy, and a constraint is given for the maximum equivalent plastic strain at the fixed end. Globally optimal solutions are searched by a simulated annealing, which is successfully combined with a commercial finite element analysis code. It is shown that the energy dissipation capacity is significantly improved by optimizing the flange shape.
Keywords: *Shape Optimization, H-Beam, Flange, Plastic Energy Dissipation, Simulated Annealing*

1 Introduction

Recent rapid developments of computer technology and optimization algorithm enabled us to optimize real-world structures under constraints that are required in design practice. In addition to optimizing structural system, it is possible to find optimal shapes of structural components or parts discretized to finite elements; e.g., shapes of suspension of automobiles, airfoil wings, and so on. In the civil engineering field, however, shape optimization of the structural components has not been well investigated. In this study, we present an approach to shape optimization of the flange of an H-beam to maximize the plastic energy dissipation capacity.

In response to brittle fracture near the beam-to-column flange groove welds in the 1994 Northridge earthquake, a wide variety of beam-to-column connection concepts have been developed. Among them, the Reduced Beam Section (RBS) connection attained much popularity, particularly in the West Coast of U.S., and various shapes such as constant cuts, tapered cuts and circular cuts have been investigated [1,2].

In an RBS connection, portions of the beam flanges are selectively trimmed in the region adjacent to the connection in order to force a plastic hinge to be located within the reduced section, and thereby reduce the likelihood of fracture occurring at the flange groove welds and the region of the surrounding base metal. Optimizing the shape of the RBS cut can increase the energy dissipation capacity of the connection, and further minimize the likelihood of fracture in the flange of the RBS by realizing widely distributed plastification with less maximum plastic strain.

Optimization of elastoplastic structures has been extensively investigated in 1990s including sensitivity analysis of path-dependent problems [3,4]. Approximation methods such as response surface method are currently applied to an elastoplastic optimization problem, because it usually has multiple local optima and application of gradient-based approach is not desirable. Heuristic approaches have been developed to obtain approximate optimal solutions within reasonable computational cost, although there is no theoretical proof of convergence [5]. The Simulated Annealing (SA) is categorized as a single-point-search heuristic approach that is based on local search and improves ability of finding globally optimal solution by allowing the move to a non-improving solution with a specified probability.

In this study, we present a method of optimizing shapes of beam flanges based on SA, which is successfully combined with a commercial finite element analysis code called ABAQUS [6]. The objective function to be maximized is the dissipated energy under forced displacement. Constraints are given for the maximum equivalent plastic strain. It is shown in the numerical examples that the energy dissipation capacity can be significantly improved by optimizing the shape of the flange.

2 Optimization problem and optimization method

Consider a cantilever beam that represents a half of a beam in a building frame. Optimal flange shapes are to be found under the static loading condition defined by forced displacement at the free end. The beam is discretized into finite elements. The shape of the flange is defined by a cubic spline curve, and the design variables are the locations of the control points. Let $\mathbf{x}$ denote the vector consisting of the variable coordinates of the control points. The upper and lower bounds for $\mathbf{x}$ are denoted by $\mathbf{x}^{\mathrm{U}}$ and $\mathbf{x}^{\mathrm{L}}$, respectively. A component of a vector is indicated by subscript; i.e., $\mathbf{x} = \{x_i\}$.

The objective function is the dissipated energy $E(\mathbf{x})$ throughout the loading history. Since the final deformed state is defined by the displacement, an unfavorable local plastification can be avoided by maximizing $E(\mathbf{x})$. The upper bound $\bar{\varepsilon}^{\mathrm{p}}$ is given for the maximum equivalent plastic strain ε^{p} among the elements at the fixed end to prevent fracture at the beam-to-column flange groove welds. Hence, the optimization problem is formulated as

$$\begin{aligned} &\text{Maximize} && E(\mathbf{x}) \\ &\text{subject to} && \varepsilon^{\mathrm{p}} \le \bar{\varepsilon}^{\mathrm{p}} \\ & && x_i^{\mathrm{L}} \le x_i \le x_i^{\mathrm{U}}, \quad (i = 1, \cdots, m) \end{aligned} \tag{1}$$

where m is the number of design variables.

The SA for continuous variables by Goffe *et al*. [7] is used for optimization. The main feature of this method is that it controls the size of the most promising area defined by the maximum distance to the neighborhood solutions, which is initially moderately large, gradually adjusted to an appropriate value, and finally reduced to reach the global optimum. The constraint $\varepsilon^{\mathrm{p}} \le \bar{\varepsilon}^{\mathrm{p}}$ is incorporated by a penalty function approach.

4 Optimization results

Optimal flange shapes are found for a wide-flange cantilever beam with a cross-section of H−150×150×7×10 as shown in Fig. 1.. The length of the cantilever beam is 700 mm. The normal flange shape is shown in Fig. 2. The flange width is to be varied at the 300 mm region from the welded section (fixed end). The variation is modeled by a cubic spline curve and maintains the symmetry with respect to the flange center line. The control points are given in Fig. 2. The location of the control point 6 is fixed, and the points 0–5 can move only in the *y*-direction; i.e. the number of design variables is 6 considering the symmetry condition with respect to the *x*-axis. The upper and lower bounds of the variables are 75 mm and 25 mm, respectively. Hence, only reduction is allowed for the flange width at the control point. Optimization is to be carried out to maximize the dissipated energy under static load up to the displacement 14 mm at the free end; i.e., the average deformation angle is 0.02.

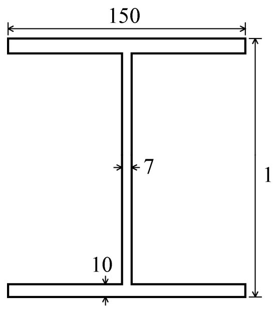

Figure 1. Flange cross-section.

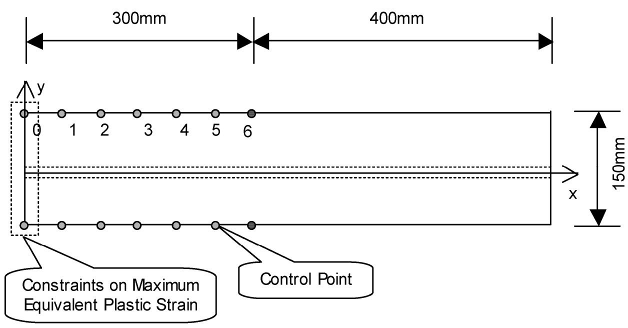

Figure2. Normal flange shape.

Elastoplastic analysis is carried out by ABAQUS Ver. 6.5.1 [8]. The S4R element, which is a 4-node quadrilateral thick shell element with reduced integration and a large-strain formulation, is used for modeling. The total numbers of elements and freedom of displacement are 504 and 3306, respectively. The elastic modulus is 2.05×10^5 N/mm^2 and Poisson's ratio is 0.3. The yield stress is 235.0 N/mm^2 and the hardening ratio is 0.001. The kinematic hardening with Prager's rule is adopted.

ABAQUS analysis is iteratively called from the SA algorithm. As shown in Fig. 3, the SA program generates new coordinates of the control points, which are the design variables of the optimization problem. This information is transmitted to ABAQUS preprocessing module that creates the beam model. The entire preprocessing module is controlled by a Python script language [8] that serves as the programming interface of ABAQUS. The control script consists of the following six steps:

1. Two parts, i.e., a flange part and a web part, are created. The cutout shape of the flange is determined using a cubic spline curve in reference to the control points.
2. Materials and section geometries are defined, and assigned to respective parts.
3. Two instances of the flange part, which represents the upper and lower flanges, and a instance of the web part are imported to form an assembly. The assembly is further merged to a single beam assembly.
4. Boundary and loading conditions are defined for the analysis.
5. The beam assembly is discretized to S4R quadrilateral shell element.
6. An analysis job is submitted to ABAQUS.

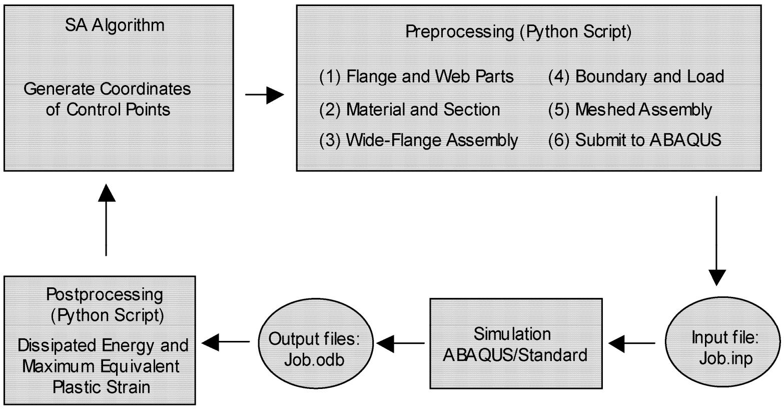

Figure 3. Flowchart of ABAQUS analysis.

In the analysis, ABAQUS/Standard is used for solving the numerical problem defined in the 'inp' file created by ABAQUS preprocessing module. An 'odb' file, which contains the analysis results, is generated. A postprocessing module also written by the Python script language is used to extract the necessary data such as the dissipated energy and the maximum equivalent plastic strain near the beam-column connection from the 'odb' file. The data are returned to the SA program for the new round of iteration. A PC with Intel Xeon 3.4 GHz CPU and 2GB RAM is used for the computation.

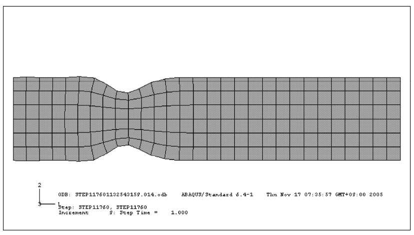

(a) Case 1

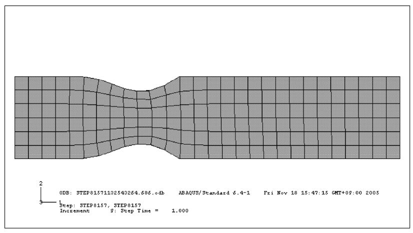

(b) Case 2

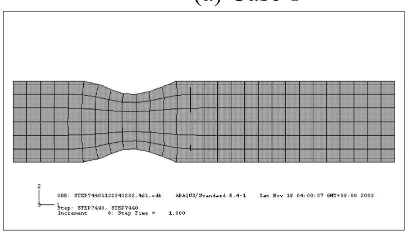

(c) Case 3

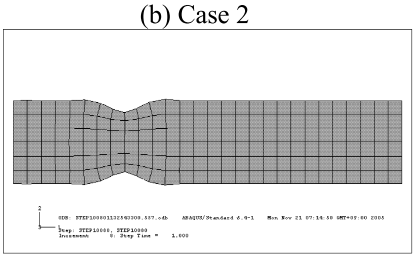

(d) Case 4

Figure 4. Optimal shapes for Cases 1–4.

The Optimal shapes for Cases 1–4 corresponding to $\bar{\varepsilon}^{\mathrm{p}} = 0.001$, 0.002, 0.004 and 0.008 are shown in Figs. 4(a)–(d). Basically, the optimal shapes share a similar pattern featured with a single concave region, which has two functions: (1) shift the maximum deformation from the welded section to the middle sections, and (2) increase the plastification area for the specified average deflection angle. It should also be noted from Fig. 4 that the specific concave shapes strongly depend on the value of $\bar{\varepsilon}^{\mathrm{p}}$. Obviously, larger reduction of the flange width is needed for smaller value of $\bar{\varepsilon}^{\mathrm{p}}$ to suppress the deformation at the welded section for the specified deflection at the free end.

Figs. 5(b)–(e) show the distributions of the von Mises stress of the beams with concave flanges for Cases 1–4, respectively, where darker color represents larger values. For the comparison purpose, the distribution of the von Mises stress and the equivalent plastic strain of normal beam with uniform flange width (referred to as Case 0 hereafter) are also plotted in Fig. 5(a). Distributions of equivalent plastic strain are also plotted in Figs.6(a)–(e). It is seen from the figures that the maximum equivalent plastic strain of Case 0 exists at the welded section, whereas it is successfully shifted to the middle section at the concave region for Cases 1-4. The distribution of the von Mises stress shows that the lengths of the plastification region of Cases 1-4 are longer that that of Case 0. This is particularly because the optimal concave shape allows longer plastified region by realizing a smooth deformed shape against the specified average deflection angle. Owing to the enlarged lengths, the total plastified areas of the flange of Cases 1-4 are not much smaller than that of Case 0, although the concavity decreases the flange width of the plastified region.

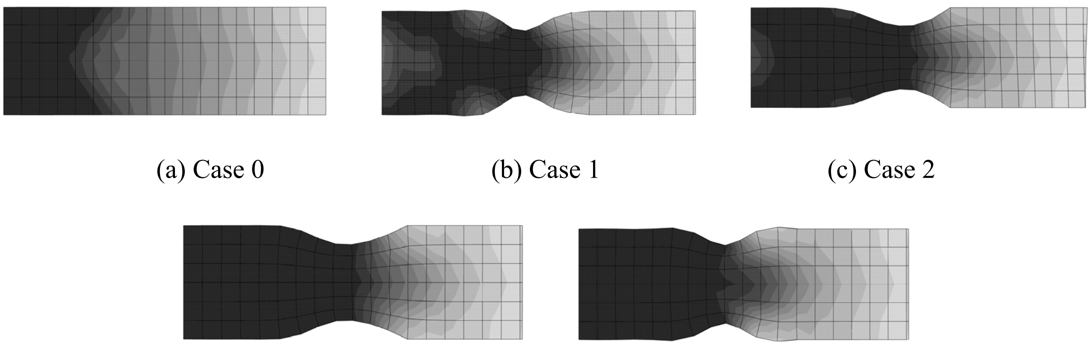

(a) Case 0 (b) Case 1 (c) Case 2

(d) Case 3 (e) Case 4

Figure 5. Distribution of von Mises stress.

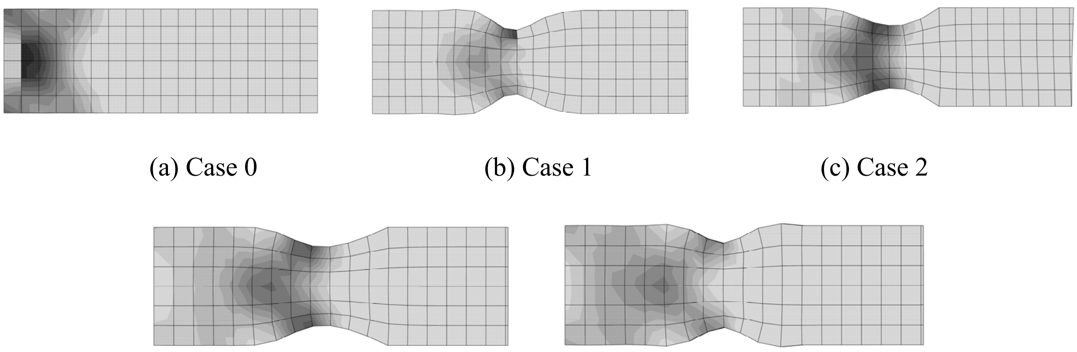

(a) Case 0 (b) Case 1 (c) Case 2

(d) Case 3 (e) Case 4

Figure 6. Distribution of equivalent plastic strain.

The dissipated energy E and the maximum equivalent plastic strain ε^{p} at the fixed end are shown in Table 1, where the average deflection angle reaches 0.02, and the results are listed for the optimal solutions of Cases 1–4. Apparently, the dissipated energy decreases with the decrease of allowable maximum equivalent plastic strain; i.e., the objective function is smaller for stricter constraints in a maximization problem. For the comparison purpose, the values of E and ε^{p} for Case 0 are also listed in Table 1. It is seen that the dissipated energy of Case 0 is not much different with those of Cases 1-4, whereas its maximum equivalent plastic strain is significantly larger compared to those of Cases 1-4. For instance, almost the same (with a difference not greater than 5%) dissipated energy of Case 0 is achieved by the optimal shape for Case 4 with less than half value of ε^{p} (0.008 for Case 4 and 0.017 for Case 0).

Table 1. Dissipated energy E and maximum equivalent plastic strain ε^{p} at the connection.

Case (ε^{p})	E	ε^{p}
Case 0 (no limit)	950	0.017
Case 1 (0.001)	875	0.001
Case 2 (0.002)	893	0.002
Case 3 (0.004)	900	0.004
Case 4 (0.008)	912	0.008

Table 2. Dissipated energy E of the normal beam considering the upper bound ε^{p} for the equivalent plastic strain at the fixed end.

ε^{p}	E	rotation angle
0.001	36	0.006
0.002	84	0.007
0.004	188	0.008
0.008	404	0.012

To further demonstrate the effect of flange shape optimization, the dissipated energy E and the allowable average deflection angle of the normal beam for $\bar{\varepsilon}^{\mathrm{p}} = 0.001$, 0.002, 0.004 and 0.008 are listed in Table 2. It can be observed by comparing Tables 1 and 2 that the dissipated energies of normal beams are far smaller than those of the optimal beams for the same value of $\bar{\varepsilon}^{\mathrm{p}}$. For $\bar{\varepsilon}^{\mathrm{p}} = 0.008$, e.g., the dissipated energy is about half of the optimal value (Case 4 in Table 1). Hence, the energy dissipation capacity is significantly increased by optimization.

The resulting average deflection angles of the normal beam at which $\bar{\varepsilon}^{\mathrm{p}} = 0.001$, 0.002, 0.004, and 0.008 are 0.006, 0.007, 0.008 and 0.012, respectively, as shown in Table 2, which are all significantly smaller than 0.02 for the optimal solutions. Contrary, if the normal beam is deformed to 2% average deflection angle, then the value of ε^{p} is 0.017 (Case 0 in Table 1), which is much larger than the upper bound for the optimal beams. Therefore, the beam with optimal flange shape is able to avoid large equivalent plastic strain at the welded section, so that its deformation capacity increases significantly.

The reaction forces of the normal and optimal beams are plotted in Fig. 7 with respect to the average deflection angle. It can be confirmed that a smaller $\bar{\varepsilon}^{\mathrm{p}}$ leads to a weaker beam in terms of initial stiffness and strength. However, they are only slightly reduced by optimization.

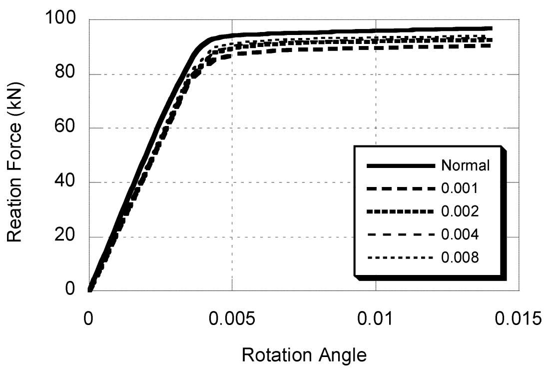

Figure 8. Force displacement relation.

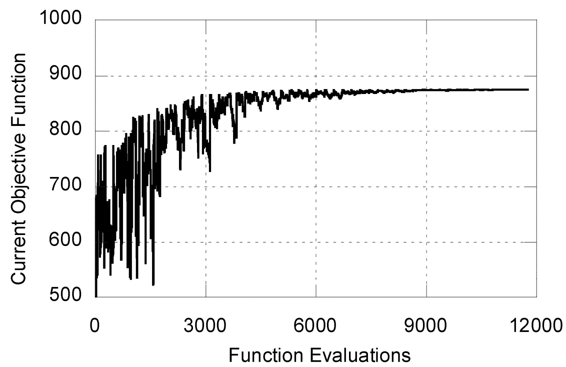

Figure 9. History of objective function by SA.

The convergence property of the objective function is shown in Fig. 9 for Case 1. As is seen, a large reduction of the objective value is allowed in the initial stage, and the objective value gradually converges to the optimal value. Note that almost optimal solutions are found within 6000 analyses. The total number of analysis is 11761 for Case 1, and the elapsed time for optimization is 63.06 hours (20 sec. per analysis). However, only 15% is used for analysis, and remaining portion of the time is; 5% for ABAQUS preprocess, 5% for ABAQUS postprocess, 75% for ABAQUS license checking, and the time used for SA algorithm is negligible.

3 Conclusions

Optimal flange shapes have been found for an H-beam under forced displacement. The objective function to be maximized is the plastic dissipated energy. The constraint is given for the maximum equivalent plastic strain at the welded section (fixed end) at the final state so that the forced displacement reaches a specified value at the free end. The conclusions drawn from this study are summarized as

1. Optimal shapes can be successfully obtained by SA in conjunction with a commercial finite element analysis code.
2. The optimal shape strongly depends on the upper bound of the equivalent plastic strain, which is to be specified in practice based on the performance required for each frame.
3. The optimization results under monotonic loading condition show significant improvement of the energy dissipation capacity compared with the normal beam with uniform flange width.

Acknowledgments

Financial support of Grants-in-Aid for Scientific Research (No. 17360270 and No. 16-4364) by MEXT, Japan, is gratefully acknowledged.

References

1. N. R. Iwankiw and C. Carter, The dogbone: a new idea to chew on, Modern Steel Constr., Vol. 36(4), pp. 18-23., 1996.
2. E. P. Popov, T. S. Yang and S. P. Chang, Design of steel MRF connections before and after the 1994 Northridge Eearthquake, Eng. Struct., Vol. 20(12), pp. 1030-1038, 1998.
3. M. Kleiber, Parameter Sensitivity in Nonlinear Mechanics, John Wiley & Sons, 1997.
4. M. Ohsaki and J. S. Arora, Design sensitivity analysis of elasto-plastic structures, Int. J. Num. Meth. Engng., Vol. 37, pp. 737-762, 1994.
5. C. Reeves, Modern Heuristic Techniques for Combinatorial Problems, McGraw-Hill, New York, 1995.
6. ABAQUS Ver. 6.5 Documentation, ABAQUS, Inc., 2004.
7. W. L. Goffe, G. D. Ferrier and J. Rogers, Global optimization of statistical functions with simulated annealing, J. Econometrics, Vol. 60(1), pp. 65-99, 1994.
8. B. David, Python Essential Reference, New Riders Publishing, 2001.